ROYAL SOCIETY
OF CHEMISTRY

PAPER

Star-shaped poly(L-lysine) with polyester bis-MPA dendritic core as potential degradable nano vectors for gene delivery†

Smiljana Stefanovic, [a] Katie McCormick, [b,c] Sarinj Fattah, [b] Ruiari Brannigan, [d] Sally-Ann Cryan [b,c,e] and Andreas Heise *[a,c,e]

Cationic star-shaped poly(L-lysine) are efficient nanovectors for the delivery of nucleic acids (gene delivery). They are commonly obtained by the ring-opening polymerisation of L-lysine *N*-carboxyanhydrides (NCA) from multifunctional amine initiators such as dendrimers. To date, commonly reported dendritic precursors are non-degradable which can cause dose dependant cytotoxicity *in vivo*. Herein, we present a new synthetic route for the preparation of star-shaped poly(L-lysine) from ammonium terminated 2,2-bis-(hydroxymethyl)propionic acid (bis-MPA) dendrimers. A range of well-defined star polypeptides with exceptionally low dispersities ($Đ_M$ < 1.05) was obtained by varying the dendrimer generation and adjusting the monomer to initiator feed ratio. The ability of efficient dendrimer core degradation was confirmed under physiological and basic conditions. Moreover, preliminary pDNA complexation studies demonstrate successful polyplex formation between the gene cargo and the star poly(L-lysine). The results suggest that the bis-MPA star poly(L-lysine) platform is a promising fully degradable alternative to leading non-degradable polymeric vectors.

Introduction

Gene therapy has long been seen as a potential solution to previously unmet clinical needs.[1] To realise the immense possibilities presented by nucleic acid-based therapeutics, the development of effective and safe delivery vehicles (vectors) is critical.[2] Nucleic acids are large, negatively charged molecules and are rapidly cleared by circulating nucleases in the body. Suitable vectors must not only protect the gene cargo against hydrolysis but also efficiently deliver them intracellularly. Positively charged polymers are poised to form stable complexes (polyplexes) with nucleic acids and have been widely investigated as non-viral gene vectors.[1] Cationic polymers including polyamidoamine (PAMAM) dendrimers and poly(ethylene imine) (PEI) have seen some success for *in vitro* gene delivery but underperform *in vivo*, which is a barrier to clinical translation.[3–7] One critical drawback of these synthetic polyamines is their dose dependent cytotoxicity.[8–10] While improved stability and easier scale-up is recognised as a benefit of polymeric vectors, it is indeed surprising that their major advantage, *i.e.* the greater flexibility in structural design and the ability to easily modify them, has not been utilised to any large extend to overcome these drawbacks.

We recently began to investigate star-shaped poly(L-lysine) (PLL) as gene delivery vectors.[11,12] Well-defined star-shaped PLL was readily prepared *via* controlled ring opening polymerisation (ROP) of amino acid-derived *N*-carboxyanhydrides (NCAs) by initiation from the primary amino groups of poly(propylene imine) (PPI) dendrimers.[13] Our research has shown that the adaptability of the macromolecular architecture is a critical advantage when optimising delivery performance to best meet the nature of the gene cargo and the clinical target. Star-shaped PLL has since been successfully applied for the delivery of advanced gene therapeutics in pre-clinical *in vitro* and *in vivo* models. The versatility in design enabled easy tailoring of the technology for delivery of gene therapeutics with different physicochemical properties. For example, a star PLL system was used to form gene nanomedicines with plasmid DNA (pDNA) to effectively transfect mesenchymal stem cells as

[a]Department of Chemistry, RCSI University of Medicine and Health Sciences, Dublin 2, Ireland. E-mail: andreasheise@rcsi.ie
[b]School of Pharmacy and Biomolecular Sciences, RCSI University of Medicine and Health Sciences, Dublin 2, Ireland
[c]AMBER, The SFI Advanced Materials and Bioengineering Research Centre, RCSI, Dublin 2, Ireland
[d]School of Chemical Sciences, Dublin City University, Collins Avenue, Whitehall, Dublin 9, Ireland
[e]Science Foundation Ireland (SFI) Centre for Research in Medical Devices (CURAM), RCSI, Dublin 2, Ireland
†Electronic supplementary information (ESI) available: bis-MPA dendrimer synthesis and characterisation, additional polymer NMR and GPC analysis. See DOI: https://doi.org/10.1039/d3py00346a

well as for siRNA and pDNA delivery to epithelial cells to treat conditions such as cystic fibrosis (CF).[11,14] Incorporated into gene activated scaffolds and implanted into a rat calvarian defect model (bone defect), star PLL nanomedicines were found to significantly enhance bone regeneration after just four weeks.[15] These materials were found to be more efficient at delivery of gene cargoes to difficult-to-transfect cells, while exhibiting enhanced biocompatibility when compared to leading commercial vectors.[16] One concern of the current star PLL delivery vector technology is the incorporation of dendritic PPI. PPI dendrimers show a low degree of hydrolytic degradation which could result in prolonged circulation in the blood stream and potential bioaccumulation in the liver.[17] Moreover, PPI dendrimer synthesis is tedious, requiring high temperature and pressure, which limits easy access to the material.[18] Other multivalent polymers have been used as a core in the preparation of star-shaped polypeptides, including polyamidoamine (PAMAM) dendrimers but all of them suffer from similar drawbacks as PPI.[19–24]

Conversely, 2,2-bis-(hydroxymethyl)propionic acid (bis-MPA) based dendrimers are an economical polyester-based alternative to PPI dendrimers, because of their non-demanding and inexpensive preparation. A main advantage is their proven biodegradability, biocompatibility, and low toxicity. They undergo pH triggered hydrolytic degradation resulting in low molecular weight products that can easily be eliminated from the body.[25] Recently, Garcia-Gallego *et al.* proposed a concept of fluoride promoted esterification chemistry to prepare bis-MPA dendrimers.[26] That concept is based on a straightforward synthetic method, where 1,1′-carbinyldiimidazole (CDI) is used as a coupling agent for activation of acetonide-protected bis-MPA and caesium-fluoride (CsF) as a catalyst, allowing full conversion of the building blocks. Bis-MPA dendrimers thus combine a number of benefits, which makes them interesting alternatives as core materials for the star PLL platform. However, their feasibility as initiators for NCA ROP has never been investigated. Here we present a systematic study into the design of fully degradable star PLL based on a bis-MPA dendritic core. We demonstrate the flexibility in the design of well-defined star polypeptides with different number of arms and molecular weights. Moreover, preliminary data on degradation and plasmid DNA complexation are presented.

Experimentals

Materials and methods

All chemicals and solvents were purchased from Sigma Aldrich and used as received unless otherwise noted. Syntheses of Lysine NCA and alanine bis-MPA initiators were carried out following literature procedures (details provided in the ESI†).[26–28] Amberlyst A21 resin was purified following literature.[27] 1,1-Carbonyldiimidazole (CDI) was stored in a desiccator due to moisture sensitivity. Attenuated total reflection (ATR) FT-IR spectroscopy was performed using a PerkinElmer Spectrum 100 in the spectral region of 650–4000 cm^{-1}. Proton (^{1}H) and

carbon (^{13}C) nuclear magnetic resonance (NMR) spectra as well as diffusion ordered (DOSY) spectra were recorded using a Bruker Avance 400 (400 MHz) spectrometer at room temperature in d-TFA, CDCl$_3$, CD$_3$OD, and D$_2$O as solvents. All chemical shifts of ^{1}H and ^{13}C NMR spectra are reported in parts per million (ppm) while diffusion coefficients are reported in cm^2 s^{-1}. The obtained spectra were analysed in MestReNova 6.02 software. DOSY data were processed using the Bayesian transform method. Diffusion coefficients were calculated from intensity of methylene signal of L-lysine side chain at 2.81 ppm using a mono-exponential decay equation, which is simplified version of Stejskal–Tanner function: $I = I_0 \exp(-DZ)$ and $Z = \gamma^2 G^2 \delta(\Delta - d/3)$.[29] I is the intensity of integral (methylene signal at 2.81 ppm); I_0 is the maximum intensity, G is the gradient strength in G cm^{-1}, δ is the gradient duration in seconds and Δ is the echo delay in seconds. Z represents the argument of the exponent and it is calculated from the arrayed experimental data. Molecular weight dispersities ($Đ$) and number average molecular weights (M_n) of the polymers were determined by gel permeation chromatography (GPC). GPC was conducted in 1,1,1,3,3,3-hexafluoro-2-propanol (HFiP) using a PSS SECurity GPC system equipped with a PFG 7 μm 8 × 50 mm pre-column, a PSS 100 Å, 7 μm 8 × 300 mm and a PSS 1000 Å, 7 μm 8 × 300 mm column in series and a differential refractive index (dRI) detector at a flow rate of 1.0 mL min^{-1}. The system was calibrated against Agilent Easi-Vial linear poly (methyl methacrylate) (PMMA) standards and analysed by PSS winGPCUniChrom. All GPC samples were prepared using a concentration of 2 mg mL^{-1}, and were filtered through a 0.2 μm millipore filter prior to injection.

Synthetic procedures

Star poly-ε-carbobenzoxy-L-lysine (G1-(8)-PZLL$_5$). As a representative procedure, the NCA of ε-carbobenzoxy-L-lysine (ZLL) (500 mg, 1.63 mmol) was dissolved in 5 mL of 2.2-dimethylformamide (DMF) in a Schlenk tube. A solution of G1-(8)-NH$_3^+$ dendrimer (48 mg, 0.040 mmol) in 2 ml DMF was quickly charged *via* a syringe to the NCA solution. The reaction was carried out 72 h at 40 °C. Depending on the type of the initiator, the used molar amounts of the initiator and the monomer were adjusted to achieve the desired molecular weight of the star-shaped polypeptides. The polymer was precipitated into diethyl ether and dried under a vacuum. G1-(8)-PZLL$_5$: ^{1}H NMR (400 MHz, CDCl$_3$) δ 7.30 (d, CH$_2$–**C$_6$H$_5$**), 5.11 (s, C$_6$H$_5$–**CH$_2$**)$^{\text{PZLL}}$, 4.46 (s, –C–**CH$_2$**–O–)$^{\text{PERT/bis-MPA}}$, 4.24 (s, –CO–**CH**–NH–)$^{\text{PZLL}}$, 3.55 (s, –CO–**CH$_2$**–CH$_2$–)$^{\beta\text{-ala}}$, 3.13 (s, –**CH$_2$**–CH$_2$–NH–)$^{\text{PZLL}}$, 2.64 (s, –**CH$_2$**–CH$_2$–NH–)$^{\beta\text{-ala}}$, 1.82 (d, –**CH$_2$**–CH$_2$–NH–)$^{\text{PZLL}}$, 1.37 (d, –**CH$_2$**–CH$_2$–)$^{\text{PZLL}}$. GPC: M_n = 13 600, M_w = 14 000, $Đ$ = 1.03.

Star poly(L-lysine) G1-(8)-PLL$_5$. G1-(8)-PZLL$_5$ (380 mg) was dissolved in 5 mL of trifluoroacetic acid (TFA). A 6-fold excess with respect to ε-carbobenzoxy-L-lysine of a 33% solution of HBr in acetic acid (0.44 mL) was added slowly to the reaction. After 16 h, the solution was precipitated into diethyl ether. The precipitate was re-dissolved in methanol and precipitated twice into diethyl ether. The excess of the solvent was removed

by vacuum overnight. The polymer was dissolved in deionised water and dialysed (cut-off 3500 Da) for 2 days with a frequent change (3 to 4 times per day) of dialysate. Afterwards, the polymer was lyophilised. G1-(8)-PLL$_5$: ^{1}H NMR (400 MHz, D$_2$O) δ 4.37 (s, –CO–CH–NH–)^{PLL}, 4.31 (s, –C–CH$_2$–O–)$^{bis-MPA}$, 4.00 (s, –C–CH$_2$–O–)^{PERT}, 3.40–3.61 (d, –CO–CH$_2$–CH$_2$)$^{\beta-ala}$, 3.06 (s, CH$_2$–CH$_2$–NH)^{PLL}, 2.70 (s, –CH$_2$–CH$_2$–NH–)$^{\beta-ala}$, 1.82–1.69 (m, –CH$_2$–CH$_2$)^{PLL}, 1.61–1.40 (m, CH$_2$–CH$_2$–NH–)^{PLL}, 1.36 (s, C–CH$_3$)$^{bis-MPA}$.

Evaluation of monomer conversion. To monitor the monomer conversion, FTIR spectra of the polymerisation solutions were collected at different time intervals. The conversion of NCA was calculated from the integral intensity ratio between anhydride peak (C=O stretching) at 1793 cm^{-1} and a peak from L-Lys fingerprint region (C–H wags), at 1255 cm^{-1} which remain unchanged during the polymerisation (Fig. S21†). Quantification of the NCA conversion was calculated using equations:

$$\text{Conversion}, \% = 100 - R_t/R_0 \times 100;$$

$$R_t = I_t(1786)/I(1255), R_0 = I_0(1786)/I(1255)$$

R_t represents the intensity ratio between the bands at 1786 cm^{-1} and 1255 cm^{-1} at different time points. R_0 is the intensity ratio of the bands of the sample taken before the initiator was added into the reaction vessel.

Assessment of polypeptide degradation. Hydrolytic degradation studies were conducted on the polypeptide G3-(32)-PLL$_{10}$. Hydrolytic degradation of the bis-MPA core was performed at pH = 4.5, 7.4, and 9.5. Acidic and basic solutions were formed by adjusting the pH of deionised water using 1 M solutions of hydrochloric acid and sodium hydroxide respectively. pH = 7.4 was obtained using phosphate buffered saline (PBS) solution as a degradation media. All solutions were prepared by dissolving 30 mg of the polypeptide in 3 mL of pre-prepared media. The solutions were placed in an incubator and kept at 37 °C for 6 days. Aliquots of each solution were lyophilised and analysed by NMR and GPC.

Buffering capacity. A modified method described by Shi *et al.* was used to determine the buffering capacity of G2-(16)-PLL$_5$ and G3-(32)-PLL$_{10}$ polymers.[30] Approximately 6 mg of each polymer was dissolved in 30 ml of molecular grade water. The solution was brought to pH 11 using 0.1 N sodium hydroxide (NaOH) then titrated with 50 μl aliquots of 0.1 N hydrochloric acid (HCL). The solution was allowed to equilibrate for 60 seconds following each addition of HCL aliquots under constant stirring and the pH was recorded using a benchtop pH meter.

Encapsulation efficiency and physicochemical studies. Plasmid DNA, plasmid Gaussia Luciferase (pGlu) was used as a cargo to study the encapsulation efficiency and complexation capacity of bis-MPA-PLL star polymers. The polyplexes were formed *via* self-assembly with 2 different generations of the star polymers at several nitrogen : phosphate (N/P) ratios including, 0.5, 1, 2, 5, 10 and 20 (N/P represents the molar ratio of positively charged nitrogen (N) in the polyLys arms to

negatively phosphate (P) group present in the pGlu molecules). The concentration of pGlu remained constant at 1 μg μl^{-1}. Gel retardation assays were used to assess the encapsulation efficiency across N/P ratios in the range 0.5–20. Briefly, a 1% agarose gel (Fisher Scientific) was prepared in 1× TBE buffer (Invitrogen, USA) containing SYBR® safe nucleic acid stain (Invitrogen, USA). The gel and tray were placed in an electrophoresis tank containing 1× TBE running buffer. 20 μl of each polyplex sample containing 6× gel loading dye was carefully loaded into each well alongside an appropriately sized DNA ladder (1Kb DNA Plus Ladder, Invitrogen, Ireland). The samples were then electrophoresed at 80 V for 40 minutes then visualised using Amersham Imager RGB 600 (GE Healthcare). To explore polyplex size and zeta potential, polyplexes were prepared in 50 μl volumes and diluted to 1 ml with molecular grade water. The polyplexes were assessed for diameter (nm) using nanoparticle tracking analysis (NTA) utilising a Nanosight NS3000 (Malvern, UK), while a zeta potential measurement (mV) was performed using a Malvern Zetasizer ZS 3000 (Malvern, UK). All techniques have been previously described.[31]

Stability of polyplexes by heparin competition assay. To evaluate the stability and dissociation of polyplexes, heparin displacement assays were performed. bis-MPA-pDNA polyplexes were prepared at N/P 10 in 50 μL volumes (described above) and incubated with 1 μg–10 μg of heparin sodium at 37 °C for 60 minutes. Samples were run on a 1% agarose gel and visualized as described in previous section. Controls included a 1 kb DNA Plus ladder, uncomplexed pDNA, and polyplexes not incubated with heparin.

Results and discussion

Synthesis and characterisation of star PLL from bis-MPA dendrimers

Three generations of bis-MPA hydroxy dendrimers were prepared *via* esterification of acetonide protected bis-MPA (Scheme S1†) and pentaerythritol (PERT) as a tetrafunctional core following a literature procedure.[27] The divergent growth was accomplished by addition of bis-MPA monomer 'layer-by-layer'. Due to the unique ^{1}H NMR resonances of both bis-MPA and PERT, it was possible to confirm the successful synthesis and purity of three generations of hydroxy terminated dendrimers corresponding to 8, 16 and 32 terminal hydroxy groups (Fig. S5–S10†). Typically, controlled NCA ROP polymerisation is initiated by nucleophiles, mostly primary amines. This offers straightforward control over molecular weight through the initiator (amine) to monomer (NCA) ratio.[32] Initiation from weaker nucleophiles such as hydroxy groups is rarely reported due to their low nucleophilicity relative to primary amines. Indeed, when the direct polymerisation of ε-carbobenzyloxy-L-lysine *N*-carboxyanhydride (ZLys NCA) from the native 8-arm bis-MPA dendrimer was attempted, reactions were slow producing polymers with relatively high dispersity ($Đ_M$ = 1.35) implying an uncontrolled polymerisation (Fig. S11†). This result was

not unexpected for the initiation from a weak nucleophile, although two recent reports disclosed some success for the initiation from hydroxy groups using 1,1,3,3-tetramethyl-guanidine (TMG) as a catalyst for *N*-substituted and unsubstituted NCAs.[33,34] In the present study, a different strategy is proposed by converting the bis-MPA dendrimer hydroxy groups into amino groups. Following Stenstrom's protocol, the functionalisation of hydroxyl-terminated bis-MPA dendrimers was performed by addition of imidazole-activated *tert*-butyloxycarbonyl (Boc) protected β-alanine (Scheme S2†).[28] Subsequent deprotection by trifluoroacetic acid (TFA) yielded the three generations of amino terminated dendrimers with 8, 16, and 32 amino end groups as ammonium trifluoroacetate salts (denoted as G1-(8), G2-(16) and G3-(32)). To compare the efficiency of chemically identical, but architecturally different initiators, a commercially available second generation of bis-MPA hyper-branched polyester was purchased and post-functionalised using the same synthetic strategy as for the dendrimers (G2HB-(16)). [1H] and [13C] NMR spectra of the dendrimers and hyper-branched polymer (Fig. S12–S19†) confirmed the presence of both β-alanine and bis-MPA moieties in all samples verifying quantitative functionalisation with amino acid units. Specifically, for the G1-(8) the β-alanine methylene proton resonance at 2.81 and 3.24 ppm are clearly distinguishable from the methyl signals of bis-MPA segment at 1.32 ppm and the PERT methylene groups at 4.22 ppm. GPC results (Fig. S20†) confirmed monodisperse molecular weight distributions with increasing M_n as a function of dendrimer generation (Table S1†).

It was hypothesised that the ROP polymerisation of ZLys NCA can be directly initiated from the ammonium trifluoroacetate terminated dendrimers (Scheme 1). This was based on previous reports on NCA initiation from tertiary amino salts. The concept was first demonstrated by Dimirtov and Schlaad using hydrochloride salt of ω-amino terminated polystyrene.[35] The ammonium chloride chain ends were found to be a dormant species, while their dissociation affords the ROP of NCA through the nucleophile attack by the primary amines. The authors later proposed further modification of the procedure by introducing tertiary amines as the catalysts.[36,37] Additionally, ammonium hydrochloride salts were used in the preparation of block copolymers.[38] Tetrafluoroborate salts were also used successfully for the initiation of γ-benzyl-L-glutamate from different amines.[39,40] However, to date, the concept of using ammonium salts for the initiation of the ROP of NCAs has not been applied in the synthesis of complex polypeptides architectures. Moreover, ammonium trifluoroacetate salts have not been investigated for their ability to initiate NCA polymerisation hitherto. Successful initiation would open a straightforward route from readily obtained β-alanine functionalised bis-MPA dendrimers to star polypeptides omitting any neutralisation of the ammonium groups after Boc deprotection.

All NCA polymerisations were performed at 40 °C due to the increased dissociation rate of the ammonium salts at elevated temperatures.[41] Initially the synthesis of G1-(8)-PZLL[5] (8 arms; 5 ZLys units per arm) was carried out (Scheme 1). The monomer conversion was monitored by FT-IR spectroscopy following the NCA signature bands at 1852 and 1786 cm^{-1} attributed to the anhydride C=O group (Fig. S21†). By comparison of the 1786 cm^{-1} band intensity with that of an unchanging band at 1255 cm^{-1}, the monomer conversion was estimated. As can be seen in Fig. 1 after an initial conversion of about 30% within the first 2 h, the NCA conversion increased linearly
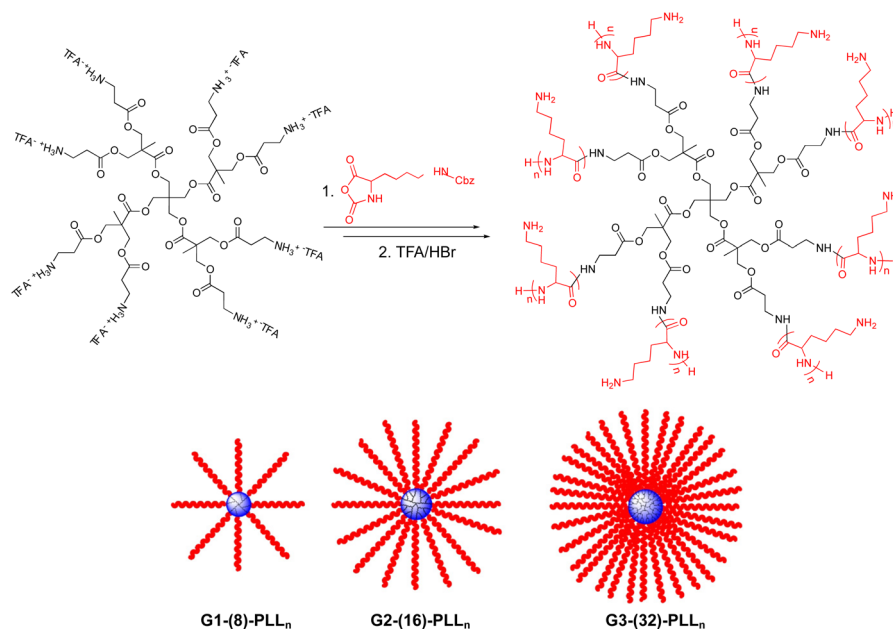
Scheme 1 Synthesis of PLL star polypeptides by NCA polymerisation using three generations bis–MPA dendrimers as the initiator.
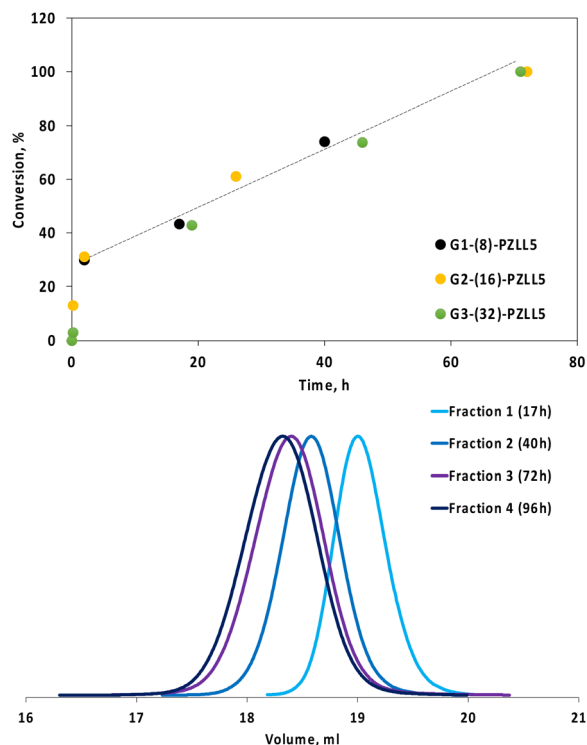
Fig. 1 Top: Conversion of ZLys NCA initiated from β-alanine ammonium trifluoroacetate bis-MPA dendrimers. Conversion was calculated from FTIR reduction of the 1786 cm⁻¹ NCA band relative to the unchanged band at 1255 cm⁻¹ (Fig. S21†). Bottom: GPC traces taken at different time points of the ZLys NCA polymerisation from the G1-(8) β-alanine ammonium trifluoroacetate bis-MPA dendrimer.
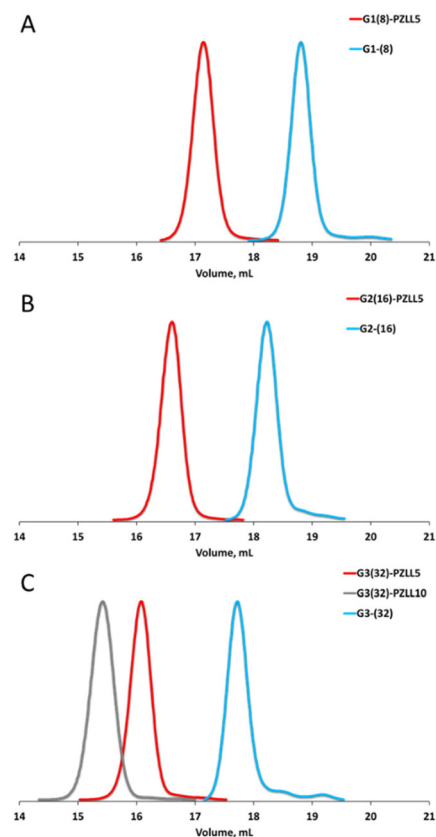

Fig. 2 GPC chromatograms of β-alanine ammonium trifluoroacetate bis-MPA dendrimers and their corresponding star PLL (HFIP, dRI detection). (A) G1-bis-MPA(8) and G1-(8)-PZLL(5), (B) G2-bis-MPA(16) and G2-(16)-PZLL(5), (C) G3-bis-MPA(32) and G3-(32)-PZLL₅, G3-(32)-PZLL₁₀.

to reach quantitative conversion after 72 h for all three samples. GPC traces of samples taken within the 72 h time interval confirmed a steady increase in molecular weight and highly symmetrical monomodal distributions verifying a well-controlled polymerisation process (Fig. 1). Extending the reaction time beyond 72 h did not result in significantly further molecular weight increase corroborating the FT-IR spectroscopic analysis. Similar results were observed for the reactions with second and third generation dendrimers and the second generation of the hyper-branched bis-MPA polymer when targeting 5 (Z)Lys units per arm. However, increasing the target degree of polymerisation (DP) per arm to 10 or more required longer reaction times.

Next, a set of star-shaped (Z)PLL with different degrees of branching and arm lengths was synthesised, whereby FT-IR spectroscopy was used to determine full monomer conversion. Three generations of (Z)PLL with 8, 16 and 32 arms and 5 Lys units per arm were targeted, denoted as G1-(8)-PLL₅, G2-(16)-PLL₅ G3-(32)-PLL₅ and G2HB-(16)-PLL₅, as well as a star-shaped polypeptide with 32 arms and 10 L-lysine units per arm, G3-(32)-PLL₁₀. GPC analysis (Fig. 2) demonstrated that all resulting star-shaped polypeptides possess a monomodal and narrow molecular weight distribution ($Đ_M$ = 1.03–1.04). For the samples with constant degree of polymerisation (DP = 5) per arm, their molecular weight (M_n^{GPC}) gradually increased with

Table 1 Star-shaped and hyper-branched PLL. Note that GPC data were obtained from the protected polymers (Z)PLL while NMR data refer to the deprotected materials

Sample	Arms	M_n^{theo} (g mol⁻¹)	$M_n^{GPC\,a}$ (g mol⁻¹)	$Đ_M{}^{b}$	DP$_{theo}$	DP$_{NMR}{}^{b}$
G1-(8)-PLL₅	8	11 670	13 600	1.03	5	5
G2-(16)-PLL₅	16	23 640	22 600	1.03	5	5
G2HB-(16)-PLL₅	16	25 694	24 900	1.15	5	6
G3-(32)-PLL₅	32	47 665	35 300	1.04	5	6
G3-(32)-PLL₁₀	32	89 636	58 400	1.03	10	11

^{a} GPC using HFiP at a flow rate of 1 mL min⁻¹ (PMMA calibration) of the protected (Z)PLL. ^{b} Degree of polymerisation per arm obtained by ¹H-NMR integration ratio between –CH₂ of alanine at 2.70 ppm and PLL at 3.06 ppm after deprotection.

increasing number of arms from 13 600 to 35 300 g mol⁻¹ (Table 1). Similarly, for the two samples with constant number of arms (32), a shift to higher molecular weight was seen when the DP per arm was increased from 5 (M_n^{GPC} = 35 300 g mol⁻¹) to 10 (M_n^{GPC} = 58 400 g mol⁻¹). Moreover, for all samples a clear shift of the traces from initiator to star polypeptide was observed (Fig. 2). The GPC trace of hyper-branched polypeptide followed the same trend, showing monodisperse molecular

weight distribution ($Đ = 1.15$) even though the initiator was less structurally uniform than the corresponding dendrimers (Fig. S24†). ^{1}H NMR spectra were in agreement with the polymer structures displaying signature peaks of the dendritic initiator and the (Z)PLL (Fig. S22†). Overall, the results emphasize a highly controlled polymerisation from the ammonium trifluoroacetate terminated multifunctional initiators giving rise to well-defined star (Z)PLL in which the molecular weight and number of arms can be readily controlled similar to our previously reported PPI core.[12] It is hypothesised that the TFA anions behave as dormant species during the polymerisation of (Z)LL NCA as previously proposed in the literature.[35,38,39]

The final synthetic step was the deprotection of the (Z)PLL arms with TFA and HBr (33 wt% in acetic acid), which was confirmed by the disappearance of the characteristic protecting group proton signals at 7.28 and 5.08 ppm (Fig. S22†). The degree of polymerisation (DP) was obtained from the ^{1}H NMR spectra of the deprotected star PLL by the calculating the integrated peak area of the $-CH_2$ signal from β-alanine at 2.70 ppm and the PLL signal at 3.06 ppm (Fig. 3). It was found that the calculated DPs were in good agreement with the targeted ones (Table 1). Notably, ^{1}H NMR analysis did not suggest any degradation under the applied conditions. The results confirm that the proposed synthetic route gives access to well defined and structurally distinct PLL star polymers.

Core degradation

The motivation for replacing the PPI dendrimer with the bis-MPA dendrimer in the star PLL platform was to impart core degradability, while retaining the ability to form polyplexes with a gene cargo. In a recent study we have demonstrated the degradability of the PLL arms on PPI 8-arm star polypeptide by the proteolytic enzyme trypsin.[42] In light of that, here we exclusively focused on investigating hydrolytic degradation of the bis-MPA core. Previously reported results of degradation studies on hydroxy terminated bis-MPA dendrimers showed
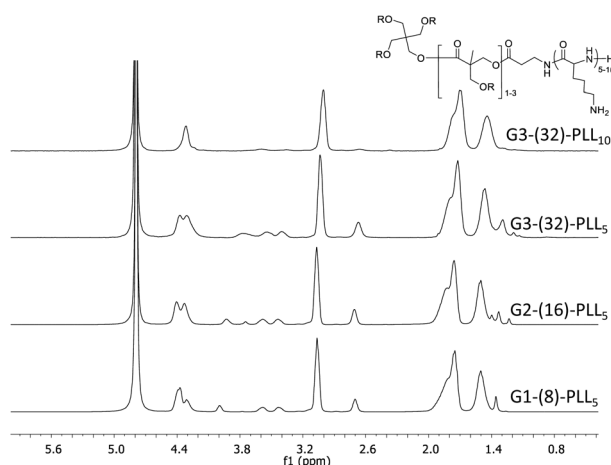
fast degradation at physiological and basic pH with a first degradation fraction at pH 7.5 appearing after only 6 h.[25] All degradation studies were standardised and carried out on G3-(32)-PLL$_{10}$ in aqueous media at a concentration 0.3 mM for 6 days at 37 °C. The star PLL was subjected to hydrolytic degradation under acidic (pH 4.5), basic (pH 9.5) and physiological (pH 7.4) conditions. At the end of the degradation experiment aliquots of the reaction solutions were removed and lyophilised. The obtained solids were subject to diffusion ordered spectroscopy (DOSY) and GPC analysis. DOSY measures diffusion coefficients of individual components in a solution mixture.[43,44] Due to diffusion being a function of molecular weight and hydrodynamic volume, we found DOSY measurements a convenient method to track the changes in molecular weight through changes in the diffusion coefficient. The DOSY contour plot of the starting sample and the materials isolated after degradation under the applied conditions is shown in Fig. 4A with diffusion coefficients listed in Table 2. The diffusion coefficient of freshly made G3-(32)-PLL$_{10}$ was 2.55×10^{-7} cm^2 s^{-1}. An increase of diffusion coefficient of the initial star polymer was recorded for the sample subjected to degradation under physiological (9.10×10^{-7} cm^2 s^{-1}) and basic conditions (8.70×10^{-7} cm^2 s^{-1}) suggesting the formation of lower molecular weight molecules due to hydrolysis. When exposed to acidic hydrolysis a smaller increase in the diffusion coeffi-

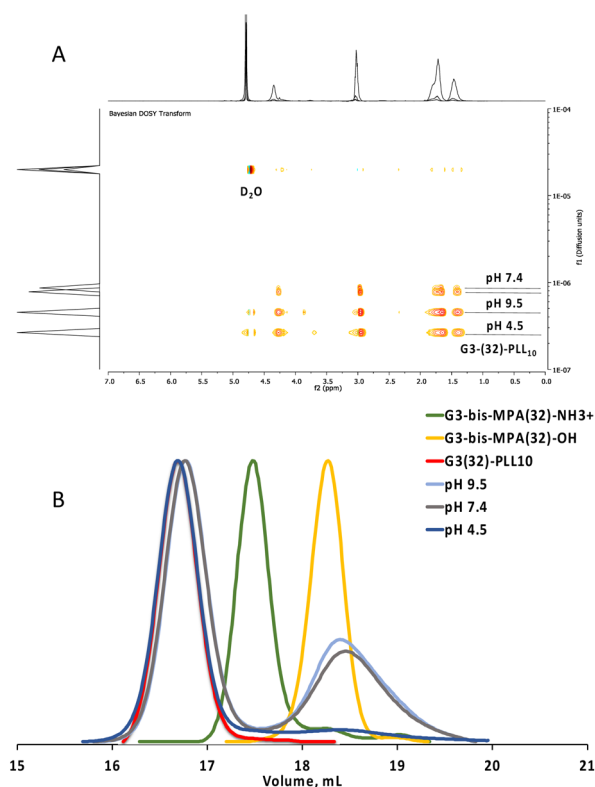**Fig. 3** ^{1}H NMR spectra of deprotected star PLL with arm length 5 and 10 in D$_2$O. Peaks used for the calculation of the degree of polymerisation (DP) are highlighted.

Fig. 4 (A) DOSY spectra of G3-(32)-PLL$_{10}$ before and after degradation at different pH. (B) GPC traces of G3-(32)-PLL$_{10}$ before and after degradation at different pH as well as hydroxy and ammonium terminated G3-bis-MPA dendrimers.

Table 2 DOSY and GPC results of the degradation studies on G3-(32)-PLL$_{10}$ under different conditions

Sample	$D^{\mathrm{NMR}\,a}$ $(10^{-7}\,\mathrm{cm^2\,s^{-1}})$	M_n^{GPC} prim.[b] $(\mathrm{g\,mol^{-1}})$	M_n^{GPC} secd.[c] $(\mathrm{g\,mol^{-1}})$
G3-(32)-PLL$_{10}$	2.55	21 630	—
pH 4.5	4.99	20 900	5500
pH 7.4	9.10	20 100	5000
pH 9.5	8.70	20 510	5150
G3-(32)-NH$_3^+$	10.87[d]	6530	—
G3-(32)-OH	16.86[e]	5310	—

[a] Diffusion coefficient in D$_2$O calculated from intensity of methylene signal of L-lysine side chain using a mono-exponential decay equation. [b] Number-average molecular weight of primary GPC trace. [c] Number-average molecular weight of secondary GPC trace. [d] Diffusion coefficient in D$_2$O calculated from intensity of methylene signal of β-alanine moiety of the dendrimer using a mono-exponential decay equation. [e] Diffusion coefficient in D$_2$O calculated from intensity of methylene signal of bis-MPA moiety of the dendrimer using a mono-exponential decay equation.

cient ($4.99 \times 10^{-7}\,\mathrm{cm^2\,s^{-1}}$) was seen. It is hypothesised that buffering by the Lys amines protonation causes the higher stability at low pH.

GPC measurements corroborate the DOSY results. Fig. 4B depicts a clear breakdown of the G3-(32)-PLL$_{10}$ starting sample evident from the second lower molecular weight maximum after degradation under basic and physiological conditions, while absent under acid conditions. Previous studies on β-alanine functional bis-MPA dendrimers showed that the bond between the β-alanine and the dendrimer is preferably hydrolysed as it is the most accessible labile bond.[45] It is reasonable that this is also the case for the star polypeptides as the PLL arms are stable under the hydrolysis conditions. While at this point somewhat speculative, this would result in the initial detachment of PLL arms which are then susceptible to further proteolytic degradation and full *in vivo* clearance.

Pharmaceutical characterisation and pDNA loading assessment

The buffering capacities of selected star PLL were investigated to determine their suitability as gene delivery vectors. The buffering capacity is a good indicator of the material's ability to facilitate a "proton sponge" effect upon cell internalisation by endocytosis.[46] From a range of polypeptides synthesised, G2-(16)-PLL$_5$ and G3-(32)-PLL$_{10}$, were selected as the reference star polypeptide materials in the following studies. As shown in Fig. 5A and B, G2-(16)-PLL$_5$ demonstrated higher buffering capacity than G3-(32)-PLL$_{10}$. G2-(16)-PLL$_5$ required 1187 ± 171 μl of 0.1 N HCL to reduce the pH to 4 *versus* G3-(32)-PLL$_{10}$ which required 681 ± 48 μl of 0.1 N HCl to reduce the pH to 4. The potential capacity of cationic polymers to facilitate gene delivery is primarily attributed to the presence of titratable amine groups within the pH range of 5–7. The presence of these amines in the material structure promotes a "proton sponge effect" in addition to the polymer's ability to volumetri-
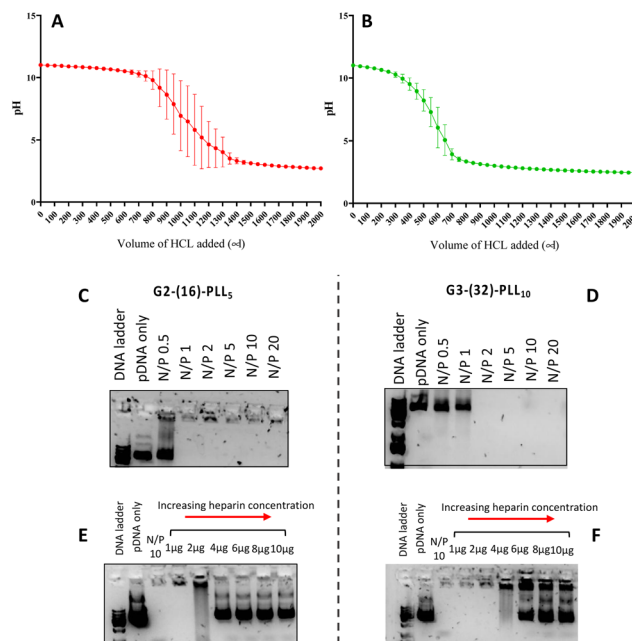

Fig. 5 Assessment of buffering capacity by acid–base titration of A: G2-(16)-PLL$_5$ and B: G3-(32)-PLL$_{10}$ alone. Data represent as the mean ± SD (*n* = 3). Effect of NP ratio on encapsulation efficiency of pGlu by G2-(16)-PLL$_5$ (C) and G3-(32)-PLL$_{10}$ (D). Lane 1: 1Kb DNA ladder, lane 2: unencapsulated pGlu (6.67 ng μl^{-1}), lanes 3–8: bis-MPA polypeptides complexed with pGLu from NP 0.5–20. Stability of polyplexes by G2-(16)-PLL$_5$ (E) and G3-(32)-PLL$_{10}$ (F). Lane 1: 1 kb DNA ladder, lane 2: unencapsulated pGlu, lane 3: control bis-MPA polyplex at NP10 and lane 4–9 polyplexes in presences of increasing heparin doses.

cally expand at lower pH 5–6 *via* the so-called "umbrella hypothesis". Together, these effects lead to endosome rupture and the prompt release of internalised polyplexes.[47] Thus the result obtained herein would suggest that G2-(16)-PLL$_5$ is more likely to function as better proton sponge in the acidic lysosomal environment once taken up by cells compared to G3-(32)-PLL$_{10}$.

To investigate the suitability of the bis-MPA star PLL polypeptides as gene delivery vectors the materials were complexed with plasmid DNA (pGLu) across a range of N/P ratios to form star PLL-pGLu polyplexes and the physicochemical properties of the polyplexes characterised. N/P represents the molar ratio of positively charged nitrogen (N) in the PLL arms to negatively phosphate (P) group present in the pGLu molecules. G2-(16)-PLL$_5$ and G3-(32)-PLL$_{10}$ polymers formed negatively charged polyplexes with pDNA at N/P 1 but positively charged polyplexes with pDNA when complexed at N/P 10 indicating complete condensation of the negatively charged pGLu at the higher N/P ratio. In addition, all polyplexes had a particle size less than 150 nm in diameter as measured with Nanoparticle Tracking Analysis (NTA) which is widely quoted as being optimal for effective nanoparticle uptake *via* endocytosis (Table 3).[48]

The encapsulation efficiency of pGLu was further confirmed using gel retardation assays. The G2-(16)-PLL$_5$ polymer

Table 3 Size and zeta potential of star PLL–pGlu polyplexes ($n = 3$)

Sample	N/P ratio[a]	Size[b] (nm)	Zeta potential (mV)
G2-(16)-PLL$_5$	1	129 ± 45	−13 ± 3
G2-(16)-PLL$_5$	10	120 ± 36	31 ± 3
G3-(32)-PLL$_{10}$	1	125 ± 54	−14 ± 3
G3-(32)-PLL$_{10}$	10	142 ± 55	33 ± 4

[a] N/P ratio is the molar ratio of positively charged nitrogen (N) arms present in the bis-MPA-PLL polymer to negatively phosphate (P) group present in the pGlu molecules. [b] Polyplex diameter (nm) measured using nanoparticle tracking analysis (NTA).

achieved complete complexation of the anionic pGluc from N/P 1 (though not at N/P 0.5) as indicated by clear lanes on the agarose gel for all N/P ratios from 1–20 (Fig. 5C). The polyplexes formulated with G3-(32)-PLL$_{10}$ achieved full complexation of the plasmid above N/P 2 but free (uncomplexed) pDNA was still evident in the gel at N/P 0.5 and N/P 1 (Fig. 5D). These results demonstrate complete complexation of pDNA at relatively low N/P ratios. It can be concluded that star bis-MPA-PLLs exhibit a similar pDNA complexation ability as the star PPI-PLLs with a similar structural composition.[11] To date, very few studies have investigated the capacity of bis-MPA dendrimers to complex with genetic materials. One study by Movellan *et al.* demonstrated for the first time the ability of bis-MPA dendrimers to condense pDNA.[49] However, very high N/P ratios were required to achieve full complexation with the dendrimer alone. In the study, a generation 2 bis-MPA with 16 terminal amino groups required a 1 : 80 000 w/w ratio, which is reported as a N/P ratio of 16 161, to fully condense the pDNA. On the other hand, the ionic analogue, ammonium-carboxylate bis-MPA, was capable of complexing pDNA at 1 : 10 w/w ratio that corresponds to N/P 100. In both cases, this is a striking difference in terms of N/P ratio *versus* our results and substantiates the significant role that the PLL arms likely play when it comes to nucleic acid complexation and condensation. In addition, results by Stenstrom *et al.* showed that second to fourth generations of ammonium trifluoroacetate bis-MPA dendrimers, with β-alanine moiety, at the periphery of the macromolecule, were able to complex small interfering RNA (siRNA) at N/P 1.5–3, which is similar to our results with pDNA and again, emphasises the importance of post-functionalisation of the bis-MPA structure for gene complexation.[50] The polyplex integrity, *i.e.* stability and ability of pDNA to dissociate from polyplexes, was further examined in the presence of a competing polyanion (heparin). Heparin is a large anionic polysaccharide found in the extracellular matrix that can compete with nucleic acid binding and disrupt polyplex stability.[51] As shown in Fig. 5E, pDNA-G2-(16)-PLL$_5$ polyplexes were destabilised in the presence of heparin at all tested concentrations, however, complete dissociation was only observed at heparin dose 2 µg or higher. While pDNA-G3-(32)-PLL$_{10}$ polyplexes were stable up to 4 µg heparin (Fig. 5F). These findings indicate that pDNA was effectively condensed by bis-MPA star polymers and that the stability of the polyplexes in the pres-

ence of a physiologically relevant molecule was dependent on the molecular structure of the bis-MPA star polypeptide. Polyplexes formed with bis-MPA star polypeptides synthesised with a greater number of arms *i.e.* G3 (32) were more stable as evidenced by the increased dose of heparin required to dissociate pDNA from these polyplexes. Similar studies were performed with PPI-based star polypeptides complexed with pDNA polyplexes and found that dissociation of pDNA was evident around the 4 µg dose of heparin.[14]

Overall, these results would suggest that different generations of star bis-MPA-PLL hybrids have the ability to effectively complex pDNA into nanoparticles that have properties suitable for cellular transfection.[52]

Conclusions

In this work, the synthesis of well-defined star-shaped PLL by ring opening polymerisation of (Z)LL NCA from three generations of bis-MPA ammonium terminated dendrimers as well as a second generation of bis-MPA hyper-branched polymer was demonstrated. The ability of efficient core degradation was confirmed under physiological and basic conditions. Moreover, preliminary pDNA complexation studies demonstrate successful polyplex formation between the gene cargo and the star PLL. The results suggest that the bis-MPA star PLL platform is a promising fully degradable alternative to leading non-degradable polymeric vectors. Additional studies in cell transfection are underway and will further inform the potential of this platform as gene vectors.

Author contributions

S. S.: investigation, methodology, writing original draft, formal analysis. K. McC.: investigation, formal analysis. S. F.: investigation, formal analysis. R. B.: supervision, writing – review and editing. S.-A. C.: conceptualisation, funding acquisition, supervision, writing – review and editing. A. H.: conceptualisation, funding acquisition, supervision, writing – review and editing.

Conflicts of interest

There are no conflicts to declare.

Acknowledgements

References

1 E. Papanikolaou and A. Bosio, *Front. Genome Ed.*, 2021, **3**, 618346.

2 K. Gersbach and C. A. Bulaklak, *Nat. Commun.*, 2020, **11**, 5820.

3 M. Mintzer and E. E. Simanek, *Chem. Rev.*, 2009, **109**, 259.

4 A. S. Chauhan, *Molecules*, 2018, **23**, 938.

5 D. Luo, K. Haverstick, N. Belcheva, E. Han and W. M. Saltzman, *Macromolecules*, 2002, **35**, 3456.

6 S. Taranejoo, J. Liu, P. Verma and K. Hourigan, *J. Appl. Polym. Sci.*, 2015, **132**, 42096.

7 A. Kargaard, J. P. G. Sluijter and B. Klumperman, *J. Controlled Release*, 2019, **316**, 263.

8 N. Shao, Y. Su, J. Hu, J. Zhang, H. Zhang and Y. Cheng, *Int. J. Nanomed.*, 2011, **6**, 3361.

9 A. Janaszewska, J. Lazniewska, P. Trzepiński, M. Marcinkowska and B. Klajnert-Maculewicz, *Biomolecules*, 2019, **9**, 330.

10 E. Haladjova, S. Halacheva, V. Posheva, E. Peycheva, M.-V. Doumanova, T. Topouzova-Hristova, J. Doumanov and S. Rangelov, *Langmuir*, 2015, **31**, 10017.

11 M. Byrne, D. Victory, A. Hibbitts, M. Lanigan, A. Heise and S.-A. Cryan, *Biomater. Sci.*, 2013, **1**, 1223.

12 M. Byrne, R. Murphy, A. Kapetanakis, J. Ramsey, S.-A. Cryan and A. Heise, *Macromol. Rapid Commun.*, 2015, **36**, 1862.

13 M. Byrne, P. D. Thornton, S.-A. Cryan and A. Heise, *Polym. Chem.*, 2012, **3**, 2825.

14 D. P. Walsh, R. D. Murphy, A. Panarella, R. M. Raftery, B. Cavanagh, J. C. Simpson, F. J. O'Brien, A. Heise and S.-A. Cryan, *Mol. Pharm.*, 2018, **15**, 1878.

15 D. P. Walsh, A. Heise, R. M. Raftery, R. Murphy, G. Chen, F. J. O'Brien and S.-A. Cryan, *Biomater. Sci.*, 2021, **9**, 4984.

16 D. P. Walsh, R. M. Raftery, I. Mencía Castañob, R. Murphy, B. Cavanag, A. Heise, F. J. O'Brien and S.-A. Cryan, *J. Controlled Release*, 2019, **304**, 191.

17 H. Kobayashi, S. Kawamoto, T. Saga, N. Sato, A. Hiraga, T. Ishimori, Y. Akita, M. H. Mamede, J. Konishi, K. Togashi and M. W. Brechbiel, *Magn. Reson. Med.*, 2001, **46**, 795.

18 E. M. M. de Brabander-van den Berg and E. W. Meijer, *Angew. Chem., Int. Ed. Engl.*, 1993, **32**, 1308.

19 J. Li, J. Li, S. Xu, D. Zhang and D. Liu, *Colloids Surf., B*, 2013, **110**, 183.

20 K. Inoue, S. Horibe, M. Fukae, T. Muraki, E. Ihara and H. Kayama, *Macromol. Biosci.*, 2003, **3**, 26.

21 H. A. Klok, J. R. Hernández, S. Becker and K. Müllen, *J. Polym. Sci., Part A: Polym. Chem.*, 2001, **39**, 1572.

22 D. Ma, Z. H. Liu, Q. Q. Zheng, X. Y. Zhou, Y. Zhang, Y. F. Shi, J. T. Lin and W. Xue, *Macromol. Rapid Commun.*, 2013, **34**, 548.

23 S. J. Lam, A. Sulistio, K. Ladewig, E. H. H. Wong, A. Blencowe and G. G. Qiao, *Aust. J. Chem.*, 2014, **67**, 592.

24 S. J. Lam, E. H. H. Wong, N. M. O'Brien-Simpson, N. Pantarat, A. Blencowe, E. C. Reynolds and G. G. Qiao, *ACS Appl. Mater. Interfaces*, 2016, **8**, 33446.

25 N. Feliu, M. V. Walter, M. I. Montañez, A. Kunzmann, A. Hult, A. Nyström, M. Malkoch and B. Fadeel, *Biomaterials*, 2012, **33**, 1970.

26 S. García-Gallego, D. Hult, J. V. Olsson and M. Malkoch, *Angew. Chem., Int. Ed.*, 2015, **54**, 2416.

27 P. Stenstrom, O. C. Andren and M. Malkoch, *Molecules*, 2016, **21**, 366.

28 P. Stenstrom, E. Hjorth, Y. Zhang, O. C. J. Andren, S. Guette-Marquet, M. Schultzberg and M. Malkoch, *Biomacromolecules*, 2017, **18**, 4323.

29 P. Groves, *Polym. Chem.*, 2017, **8**, 6700.

30 J. Shi, J. G. Schellinger, R. N. Johnson, J. L. Choi, B. Chou, E. L. Anghel and S. H. Pun, *Biomacromolecules*, 2013, **14**, 1961.

31 D. P. Walsh, A. Heise, F. J. O'Brien and S.-A. Cryan, *Gene Ther.*, 2017, **24**, 681.

32 A. R. Mazo, S. Allison-Logan, F. Karimi, N. Jun-An Chan, W. Qiu, W. Duan, N. M. O'Brien-Simpson and G. G. Qiao, *Chem. Soc. Rev.*, 2020, **49**, 4737.

33 B. A. Chan, S. Xuan, M. Horton and D. Zhang, *Macromolecules*, 2016, **49**, 2002.

34 K. Li, Z. Li, Y. Shen, X. Fu, C. Chen and Z. Li, *Polym. Chem.*, 2022, **13**, 586.

35 I. Dimitrov and H. Schlaad, *Chem. Commun.*, 2003, 2944.

36 C. D. Vacogne and H. Schlaad, *Chem. Commun.*, 2015, **51**, 15645.

37 C. D. Vacogne and H. Schlaad, *Polymer*, 2017, **124**, 203.

38 J. F. Lutz, D. Schütt and S. Kubowicz, *Macromol. Rapid Commun.*, 2005, **26**, 23.

39 I. Conejos-Sánchez, A. Duro-Castano, A. Birke, M. Barz and M. J. Vicent, *Polym. Chem.*, 2013, **4**, 3182.

40 A. Duro-Castano, R. M. England, D. Razola, E. Romero, M. Oteo-Vives, M. A. Morcillo and M. J. Vicent, *Mol. Pharm.*, 2015, **12**, 3639.

41 Y. Knobler, S. Bittner and M. Frankel, *J. Chem. Soc.*, 1964, 3941.

42 D. Skoulas, S. Fattah, D. Wang, S.-A. Cryan and A. Heise, *Macromol. Biosci.*, 2022, 2200175.

43 W. Li, H. Chung, C. Daeffler, J. A. Johnson and R. H. Grubbs, *Macromolecules*, 2012, **45**, 9595.

44 P. Groves, *Polym. Chem.*, 2017, **8**, 6700.

45 E. F. Durán-Lara, J. L. Marple, J. A. Giesen, Y. Fang, J. H. Jordan, W. T. Godbey, A. Marican, L. S. Santos and S. M. Grayson, *Biomacromolecules*, 2015, **16**, 3434.

46 J.-P. Behr, *CHIMIA Int. J. Chem.*, 1997, **51**, 34.

47 J. Nguyen and F. C. Szoka, *Acc. Chem. Res.*, 2012, **45**, 1153.

48 D. J. Gary, N. Puri and Y. Y. Won, *J. Controlled Release*, 2007, **121**, 64.

49 J. Movellan, R. Gonzalez-Pastor, P. Martin-Duque, T. Sierra, J. M. de la Fuente and J. L. Serrano, *Macromol. Biosci.*, 2015, **15**, 657.

50 P. Stenstrom, D. Manzanares, Y. Zhang, V. Cena and M. Malkoch, *Molecules*, 2018, **23**, 2028.

51 J. McCarthy, M. J. O'Neill, L. Bourre, D. Walsh, A. Quinlan, G. Hurley, J. Ogier, F. Shanahan, S. Melgar, R. Darcy and C. M. O'Driscoll, *J. Controlled Release*, 2013, **168**, 28.

52 J. Rejman, V. Oberle, I. S. Zuhorn and D. Hoekstra, *Biochem. J.*, 2004, **377**, 159.